Mechanical Systems and Signal Processing 117 (2019) 65–80

Contents lists available at ScienceDirect

Mechanical Systems and Signal Processing

journal homepage: www.elsevier.com/locate/ymssp

# Fault diagnosis of single-phase induction motor based on acoustic signals

Adam Glowacz

*AGH University of Science and Technology, Faculty of Electrical Engineering, Automatics, Computer Science and Biomedical Engineering, Department of Automatic Control and Robotics, Al. A. Mickiewicza 30, 30-059 Kraków, Poland*

ARTICLE INFO

*Article history:*
Received 22 November 2017
Received in revised form 14 July 2018
Accepted 21 July 2018

*Keywords:*
Acoustic signal
Fault
Diagnosis
Bearing
Stator
Motor

ABSTRACT

The paper presents description of bearing, stator and rotor fault diagnostic methods of a single-phase induction motor. The presented methods use acoustic signals. Five states of the single-phase induction motor were analysed: healthy motor, motor with shorted coils of auxiliary winding and main winding, motor with shorted coils of auxiliary winding, motor with broken rotor bar and faulty ring of squirrel-cage, motor with faulty bearing. A method of feature extraction of acoustic signals – SMOFS-22-MULTIEXPANDED (Shortened Method of Frequencies Selection Multiexpanded) was developed and implemented. The SMOFS-22-MULTIEXPANDED was implemented as feature extraction method of acoustic signals. Classification step was performed using the NN (the Nearest Neighbour) classifier. The proposed methods had good results for diagnosis of bearing, stator and rotor faults of the single-phase induction motor. The developed approach can find applications for fault diagnosis of other types of rotating machines.



## 1. Introduction

The number of electric rotating motor is increased every year, so it is essential to diagnose them properly. A single-phase induction motor (Fig. 1) is simple in construction, inexpensive and reliable. It finds its application in both industrial and domestic electric motors such as: drill, blowers, elevators, cordless drill, vacuum cleaner, conveyors, fans, machine tools, pumps. Many parts of the motor (rotor shaft, bearings, insulation, stator and rotor circuits) wear out depending on operating stress and operation time (Figs. 2–5). Degraded parts of electric rotating motor can cause accidents and downtimes during the operation of machine. Repair or replacement of a damaged motor costs time and money. Often it is better to repair the motor than replace it (if we have expensive machine).

Technical improvement, cost reductions and high reliability are essential for mining and fuel industries. Mining and refinery use many electric rotating motors. Stator and rotor electrical faults often appear in electric rotating motors. Such faults can damage windings of the motor permanently. There are many different approaches for detecting faults of the electric motor.

In the literature diagnostic techniques based on the analysis of defect signatures in electric currents were developed [1–6]. These techniques had high recognition efficiency. An electric signal is easy to process, because it is not so mixed together (comparing with acoustic signals).

*E-mail address:* adglow@agh.edu.pl

https://doi.org/10.1016/j.ymssp.2018.07.044
0888-3270/


**Fig. 1.** Low-cost capacity microphone and single phase induction motors.

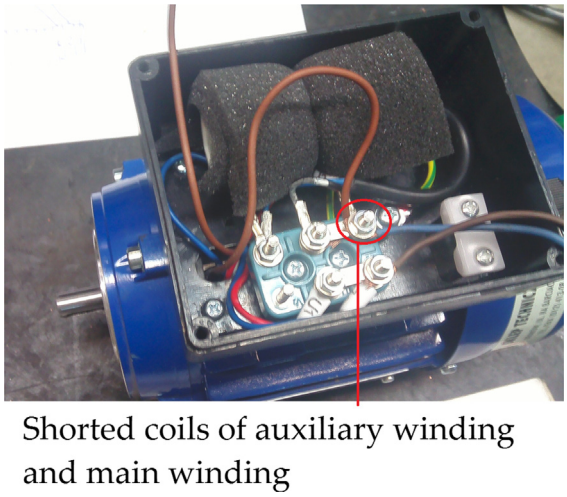


**Fig. 2.** Motor with shorted coils of auxiliary winding and main winding.

Unfortunately current signal can be used only for limited faulty states such as: shorted windings, broken bars, faulty ring of squirrel-cage [7–11]. Moreover access to the electric signal is not so easy (comparing with acoustic signals). Many articles described techniques based on vibration signals [12–16]. Techniques based on the analysis of vibration are very common used. Similarly to the analysis of electric currents, techniques based on the analysis of vibration have high recognition efficiency.

Advantages of vibration based fault diagnostic techniques are: inexpensive accelerometer, immediate measurement of the vibration signal, it is possible to analyse electrical (shorted windings, broken bars, faulty ring of squirrel-cage) and mechanical faults (bearings, rotor shaft etc.) [17–20], easy access to vibration signal. Disadvantages of vibration based fault

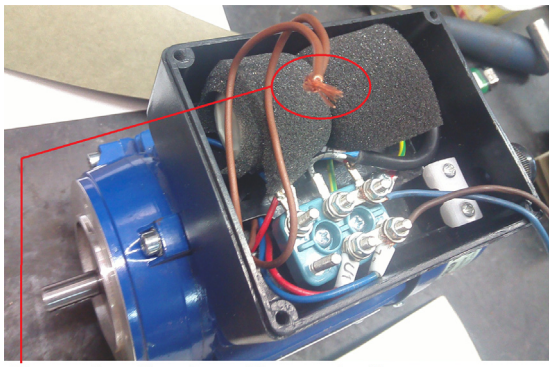


**Fig. 3.** Motor with shorted coils of auxiliary winding.

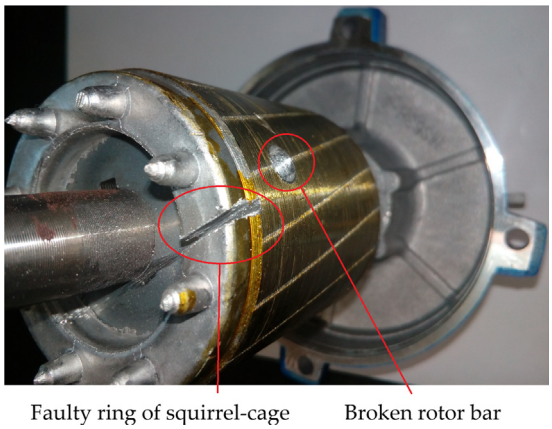


**Fig. 4.** Motor with broken rotor bar and faulty ring of squirrel-cage.

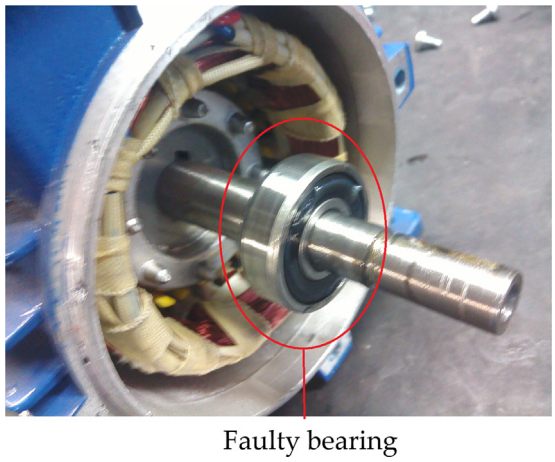


**Fig. 5.** Motor with faulty bearing.

diagnosis techniques are: set of accelerometer should be very close to the motor and set of accelerometer/data logger should be the same (measurement in the axes X, Y, Z).

In the literature there are also diagnostic techniques of rotating electric motors based on analysis of thermal images [21–24]. Measurement of thermal images is also immediate and non-invasive. The analysis of thermal images is very

efficient for fault detection. However there are some disadvantages: expensive thermal imaging camera, set of thermal camera must be the same (measurement in the axes X, Y, Z), it takes time to heat up motor, it takes time to process thermal images.

In the literature there are also acoustic based fault diagnostic techniques [25–30]. Acoustic signals of the motor are mixed by other acoustic signals (reflected signals, overlapped signals etc.). Another disadvantage of acoustic based fault diagnostic techniques is the lack of changes in the acoustic signal for some types of electrical equipment. However there are some advantages such as: easy access to acoustic signal, inexpensive microphone, it is possible to analyse electrical and mechanical faults (shorted windings, broken bars, bearings, rotor shaft etc.) [31–34]. Measurement of acoustic signals is also immediate and non-invasive. In the literature, other diagnostic techniques of electric rotating motor were developed. They are as follows: techniques based on visual analysis, techniques based on analysis of magnetic signals, lubrication analysis, techniques based on analysis of ultrasonic signals.

The paper presents description of bearing, stator and rotor fault diagnostic methods of a single-phase induction motor. The presented methods use acoustic signals. Five states of the single-phase induction motor were analysed: healthy motor (Figs. 6, 10), motor with shorted coils of auxiliary winding and main winding (Fig. 7), motor with shorted coils of auxiliary winding (Fig. 8), motor with broken rotor bar and faulty ring of squirrel-cage (Fig. 9), motor with faulty bearing (Fig. 11).

The proposed approach consists of signal processing methods: preprocessing, feature extraction, classification. An original method called the SMOFS-22-MULTIEXPANDED (Shortened Method of Frequencies Selection Multiexpanded) was used as feature extraction method of acoustic signals. The classification step was performed using the NN (the Nearest Neighbour) classifier.

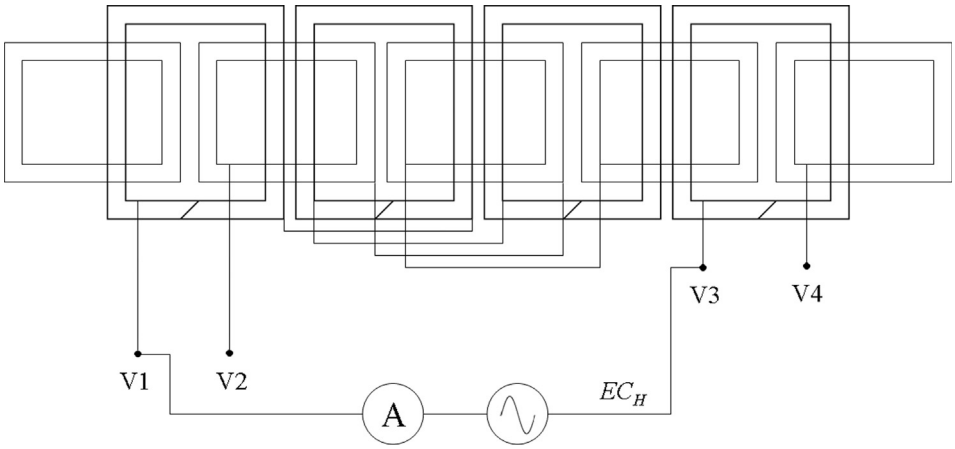


**Fig. 6.** Stator windings of the healthy motor.

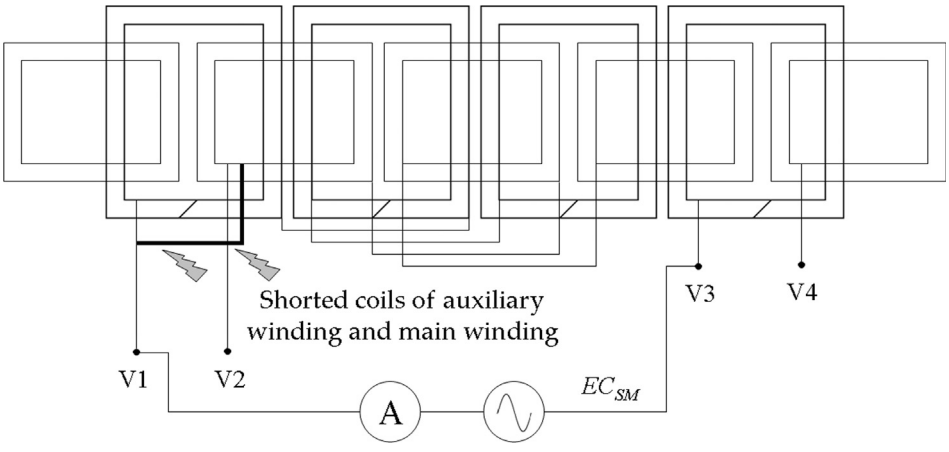


**Fig. 7.** Stator windings of the motor with shorted coils of auxiliary winding and main winding.

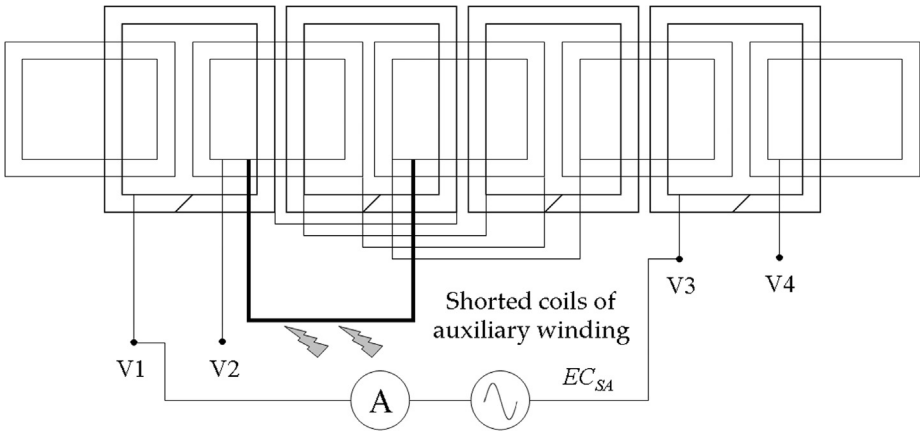


**Fig. 8.** Stator windings of the motor with shorted coils of auxiliary winding.

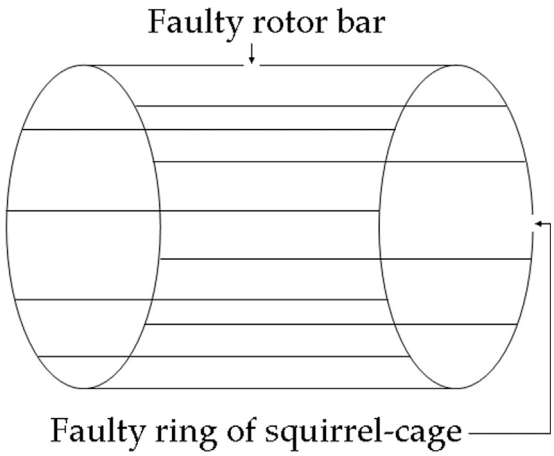


**Fig. 9.** Rotor of the motor with broken rotor bar and faulty ring of squirrel-cage.

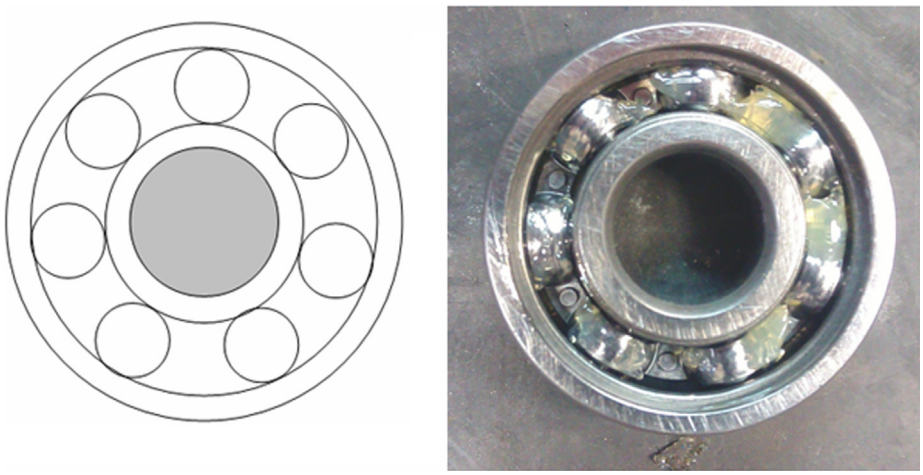

**Fig. 10.** Healthy bearing of the motor.

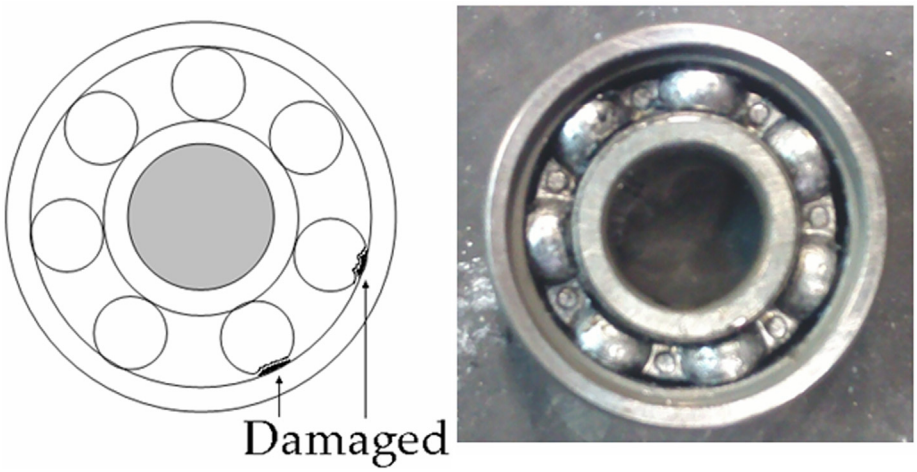


**Fig. 11.** Faulty bearing of the motor.

## 2. Proposed approach of fault diagnosis

Bearing, stator and rotor fault diagnostic methods used an analysis of acoustic signals. This analysis consisted of: measurements of acoustic signals, split of the soundtrack, amplitude normalization, FFT, SMOFS-22-MULTIEXPANDED, classification using the Nearest Neighbour classifier (Fig. 12a).

First digital voice recorder or capacity microphone with PC should be used for measurements of acoustic signals. Low-cost capacity microphone ZALMAN ZM-MIC1 can be used for this purpose. Frequency range of capacity microphone was 50–20,000 Hz. It has proper parameters for measurement of acoustic signals of analysed motors. Other types of capacitor

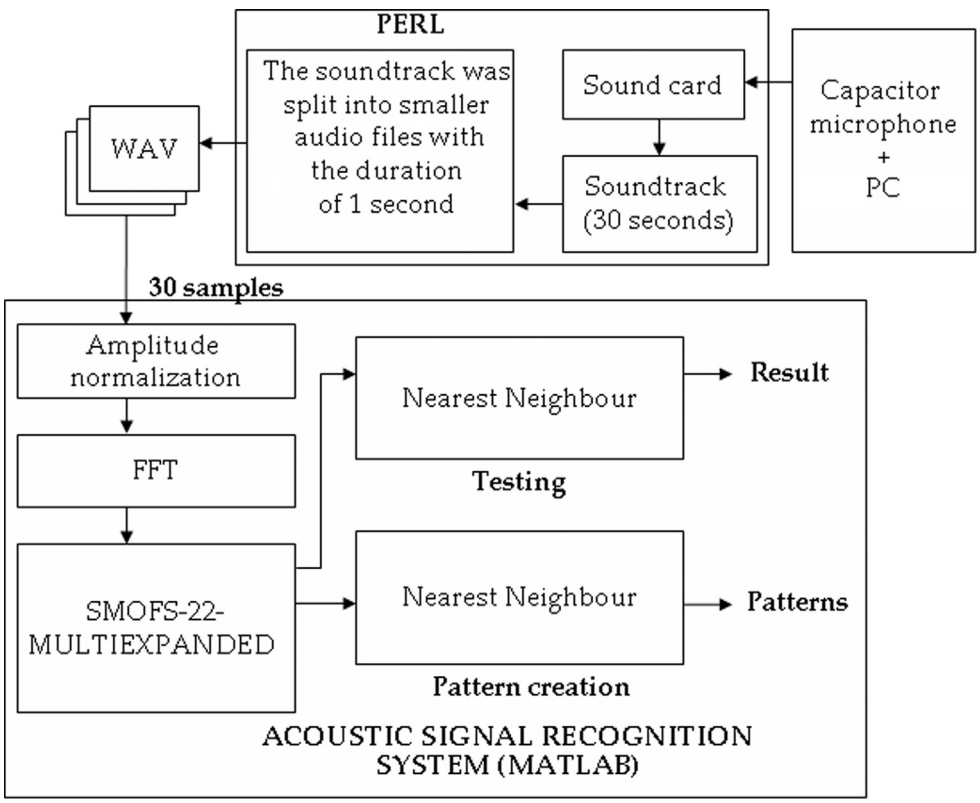


**Fig. 12a.** Proposed bearing, stator and rotor fault diagnostic methods of the single-phase induction motor using SMOFS-22-MULTIEXPANDED and acoustic signals.

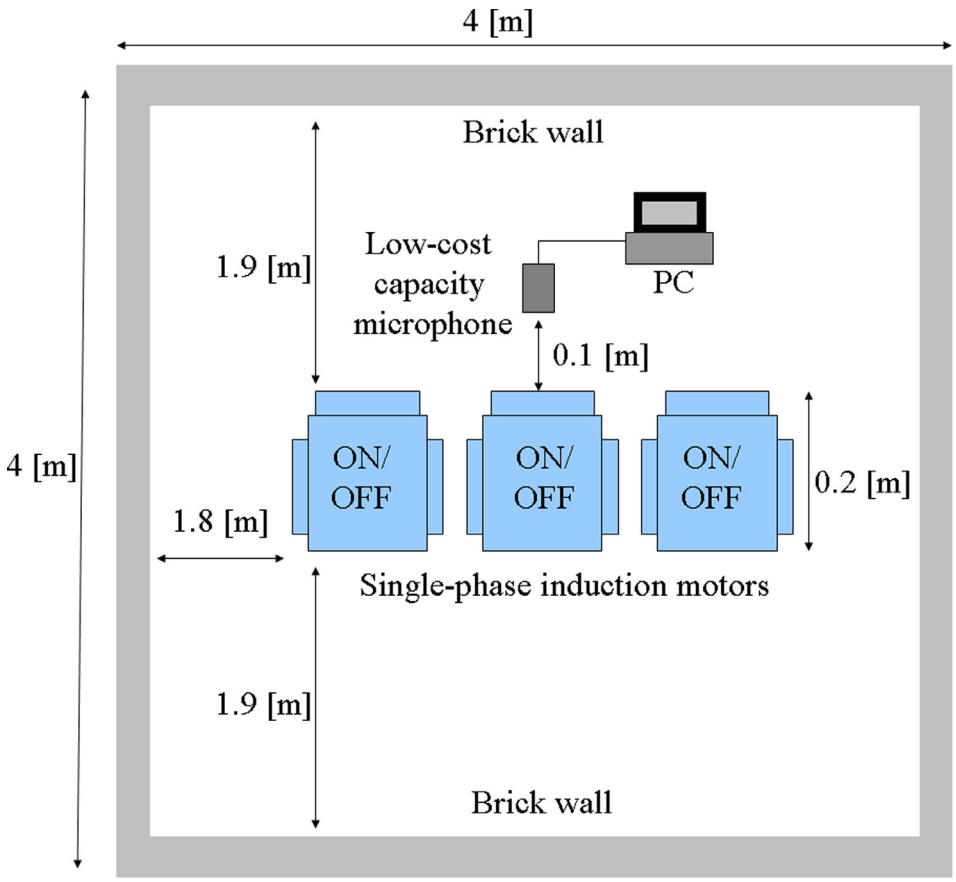


**Fig. 12b.** Experimental setup of analysis of acoustic signals of single phase induction motors.

microphones or digital voice recorders can be used for measurements. The author carried out measurements in a room of $4 \times 4$ meters. The author used one of many possibilities of measurements (Fig. 12b). Obtained format of audio data was WAVE, mono channel and sampling frequency equal to 44100 Hz.

Next acoustic data were split into 5-s data files. Data files were processed by the Hamming window and the FFT method. The FFT computed 16,384 frequency components. Next 16,384 frequency components were processed by and the SMOFS-22-MULTIEXPANDED. The SMOFS-22-MULTIEXPANDED computed 1–22 common feature vectors (Fig. 12a). The last step of proposed approach was classification using the NN classifier. It consisted of patterns creation and testing process (prediction phase). Patterns creation and testing process were computed by the NN (Nearest Neighbour) classifier. In the testing process unknown test sample (audio file) was compared with training samples using distance function (the Manhattan distance).

### *2.1. Shortened method of frequencies selection MULTIEXPANDED*

The Shortened Method of Frequencies Selection Multiexpanded (SMOFS-22-MULTIEXPANDED) was based on differences of frequency spectra of acoustic signals [35]. Construction of the motor, size, rotor speed and the analysed state of the motor were essential for analysis of acoustic signals. Frequency spectra of acoustic were different for each analysed state of the motor (healthy motor, motor with shorted coils of auxiliary winding and main winding, motor with shorted coils of auxiliary winding, motor with broken rotor bar and faulty ring of squirrel-cage, motor with faulty bearing). To extract diagnostic features, the author implemented and used the method of feature extraction SMOFS-22-MULTIEXPANDED. Seven steps of the SMOFS-22-MULTIEXPANDED were following:

1) Form vectors using frequency spectra of acoustic signals of the motor. The frequency spectrum of the healthy motor was defined as following vector $A = [a_1, a_2, \ldots, a_{16384}]$. The frequency spectrum of the motor with shorted coils of auxiliary winding and main winding was defined as vector $B = [b_1, b_2, \ldots, b_{16384}]$. The frequency spectrum of the motor with shorted coils of auxiliary winding was defined as vector $C = [c_1, c_2, \ldots, c_{16384}]$. The frequency spectrum of the motor with broken rotor bar and faulty ring of squirrel-cage was defined as vector $D = [d_1, d_2, \ldots, d_{16384}]$. The frequency spectrum of the motor with faulty bearing was defined as vector $E = [e_1, e_2, \ldots, e_{16384}]$.

2) Compute absolute values of differences of previously formed vectors: **|a-b|**, **|a-c|**, **|a-d|**, **|a-e|**, **|b-c|**, **|b-d|**, **|b-e|**, **|c-d|**, **|c-e|**, **|d-e|**.
3) Use formula (1) to select frequency components. Frequency components greater than a threshold $ThrSel_x$ are selected.

$$||FS_A| - |FS_B|| > ThrSel_x, \tag{1}$$

where $ThrSel_x$ – threshold of selection of frequency components for *x-th* iteration, $||FS_A|-|FS_B||$ – difference between frequency spectra of acoustic signals of states *A* and *B*, $FS_A$ – frequency spectrum (16384 frequency components) of state *A*, $FS_B$ – frequency spectrum (16384 frequency components) of state *B*.
4) Compute variable (threshold of selection of frequency components) $ThrSel_x$ for *x-th* iteration. The variable $ThrSel_x$ is expressed by Eq. (2):

$$ThrSel_x = \frac{\sum_{NoFC_x=1}^{NoFC_x} ||FS_A| - |FS_B||}{NoFC_x}, \tag{2}$$

$$NoFC_x \leqslant 22, \tag{3}$$

where variable $NoFC_x$ is a number of selected frequency components for *x-th* iteration (if window length equal to 32,768 the computed frequency spectrum consisted of 16,384 frequency components, $NoFC_0 = 16384$ for the first iteration, next $NoFC_0$ is decreased iteratively). If the variable $NoFC_x$ is greater than 22, the SMOFS-22-MULTIEXPANDED computes Eq. (2). If the variable $NoFC_x \leq 22$, then computations are interrupted. The SMOFS-22-MULTIEXPANDED selected 1–22 frequency components. The number of iterations *x* and the value of variable $NoFC_x$ are depended on acoustic signals. Let's analyse EXAMPLE1. We have three acoustic signals of states A, B, C. The SMOFS-22-MULTIEXPANDED computes frequency components 200, 220, 240, 260, 280, 300, 320, 340 Hz for acoustic signals of states A and B (**|a-b|**). The SMOFS-22-MULTIEXPANDED computes frequency components 210, 230, 250, 270, 290, 310, 330, 350 Hz for acoustic signals of states A and C (**|a-c|**). The SMOFS-22-MULTIEXPANDED computes frequency components 215, 220, 225, 230, 235, 240, 245, 250 Hz for acoustic signals of states B and C (**|b-c|**). Acoustic signals of states A, B, C do not have common frequency components. Frequency components 220, 230, 240, 250 Hz are found 2 times. Using of found frequency components is a good idea. However there is a problem for a higher number of considered acoustic signals. A parameter called *TCFC-MULTI* (*Threshold of common frequency components MULTIEXPANDED extension*) is introduced to analyse higher number of considered acoustic signals.
5) Set the parameter *TCFC-MULTI*. It is expressed as: *TCFC-MULTI* = (number of required common frequency components of considered training sets)/(number of computed differences). It can be noticed that the parameter *TCFC-MULTI* is essential for selection of final common frequency components. Let's consider EXAMPLE2. There are 4 training sets. Each training set has 5 acoustic signals: (FA1, FB1, FC1, FD1, FE1), (FA2, FB2, FC2, FD2, FE2), (FA3, FB3, FC3, FD3, FE3), (FA4, FB4, FC4, FD4, FE4). The SMOFS-22-MULTIEXPANDED selects frequency components for each difference in one training set: (|FA1-FB1|), (|FA1-FC1|), (|FA1-FD1|), (|FA1-FE1|), (|FB1-FC1|), (|FB1-FD1|), (|FB1-FE1|), (|FC1-FD1|), (|FC1-FE1|), (|FD1-FE1|), (|FA2-FB2|),. . ., (|FD2-FE2|), (|FA3-FB3|),. . ., (|FD3-FE3|), (|FA4-FB4|),. . ., (|FD4-FE4|) – 40 differences between frequency spectra of acoustic signals, FA1, FB1, FC1, FD1, FE1 . . . FA4, FB4, FC4, FD4, FE4 – frequency spectra of 5 states (A, B, C, D, E) of the motor. If the parameter *TCFC-MULTI* = 10/40 = 0.25, then the SMOFS-22-MULTIEXPANDED selects frequency components, which were found in 10 differences (maximum number is 40 times). For example frequency component 100 Hz were found 10 times. Frequency component 150 Hz were found 20 times. Frequency component 200 Hz were found 25 times. The SMOFS-22-MULTIEXPANDED selects 100, 150, 200 Hz (*TCFC-MULTI* = 10/40 = 0.25,). If the parameter *TCFC-MULTI* = 18/40 = 0.45, then the SMOFS-22-MULTIEXPANDED selects frequency component 150 and 200 Hz. If the parameter *TCFC-MULTI* = 30/40 = 0.75, then the SMOFS-22-MULTIEXPANDED selects 0 (*TCFC-MULTI* should be set again).
6) Find 1–22 common frequency components.
7) Form a final feature vector (1–22 found frequency components).

The implemented method SMOFS-22-MULTIEXPANDED was presented in Fig. 13.

In this paper four training sets were analysed (20 one-second samples). The differences of training vectors: **|a-b|**, **|a-c|**, **|a-d|**, **|a-e|**, **|b-c|**, **|b-d|**, **|b-e|**, **|c-d|**, **|c-e|**, **|d-e|** were shown in Figs. 14–23 (acoustic signals were generated by the single-phase induction motor with rotor speed 1390 rpm).

The SMOFS-22-MULTIEXPANDED computed 14 common frequency components – 29, 36, 42, 43, 51, 58, 61, 62, 101, 201, 483, 546, 646, 682 Hz, for *TCFC-MULTI* = 0.25. The SMOFS-22-MULTIEXPANDED computed 8 common frequency components – 29, 36, 42, 43, 51, 101, 546, 646 Hz, for *TCFC-MULTI* = 0.275. The SMOFS-22-MULTIEXPANDED computed 4 common frequency components – 36, 546, 101, 646 Hz for *TCFC-MULTI* = 0.325. There were used 20 one-second audio files for 4 training sets. Audio files were processed into common frequency components. Next feature vectors were formed using previously computed common frequency components.

Classification of feature vectors was the final step of signal processing. For this purpose the NN (Nearest Neighbour) classifier was used [36–40]. However other classification methods such as: neural network [41–47], fuzzy classifier

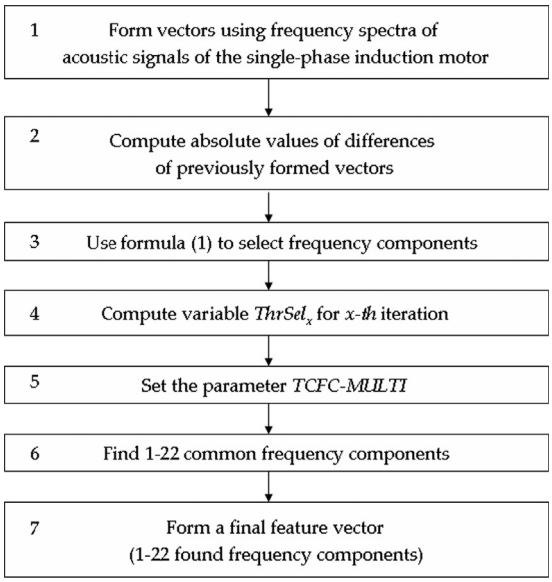


**Fig. 13.** Flowchart of the SMOFS-22-MULTIEXPANDED.

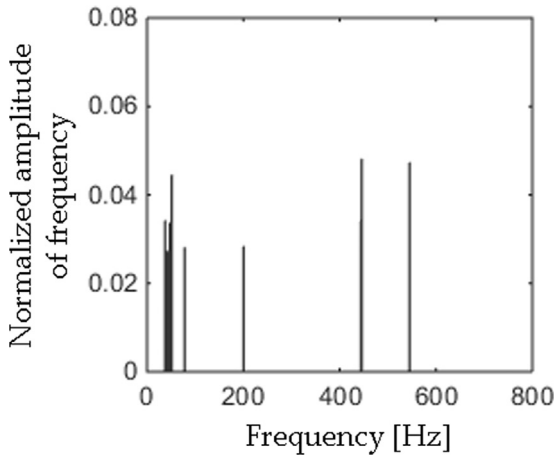


**Fig. 14.** Difference between frequency spectra of acoustic signals (|a-b|) using SMOFS-22-MULTIEXPANDED.

[48,49], Linear Discriminant Analysis, Naive Bayes classifier, Support Vector Machine [32,50,51], fuzzy c-means clustering [52] could be also used.

### *2.2. NN classifier*

The Nearest Neighbour (NN) classifier is well-known classifier [36–40]. It is robust and versatile classifier. The NN has high recognition results for multi-class problems. It is also used for many applications such as: signal processing, image processing, medical data mining, forecasting, text recognition, genomic data analysis, economic. The Nearest Neighbour (NN) is the supervised learning method. The NN uses training feature vectors which are subsequently used for the prediction phase. The NN searches training vectors and test vectors, that are the most closely resemble. Next it assigns test vector to the nearest neighbour (class). The classifier runs through the whole test set computing $d$ (similarity distance) between test feature vector and each training feature vectors. Finally, the test vector gets assigned to the class with the closest training vector. The Nearest Neighbour classifies feature vectors using similarity distance such as: Manhattan, Euclidean, Minkowski, cosine, Jaccard, Chebyshev. The Manhattan distance (4) was used for analysis of acoustic signals, because the obtained results using other similarity distances were similar. The Manhattan distance was presented as:

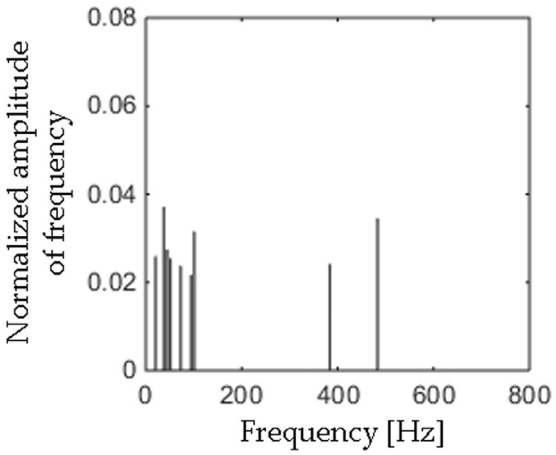


**Fig. 15.** Difference between frequency spectra of acoustic signals (|a-c|) using SMOFS-22-MULTIEXPANDED.

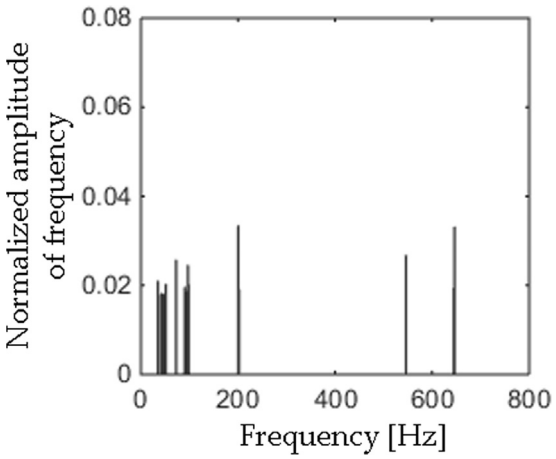


**Fig. 16.** Difference between frequency spectra of acoustic signals (|a-d|) using SMOFS-22-MULTIEXPANDED.

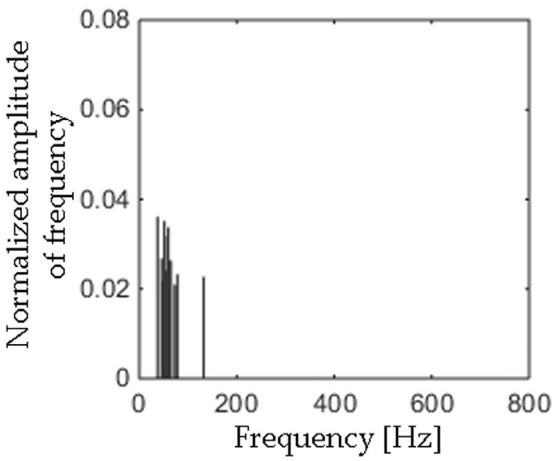


**Fig. 17.** Difference between frequency spectra of acoustic signals (|a-e|) using SMOFS-22-MULTIEXPANDED.

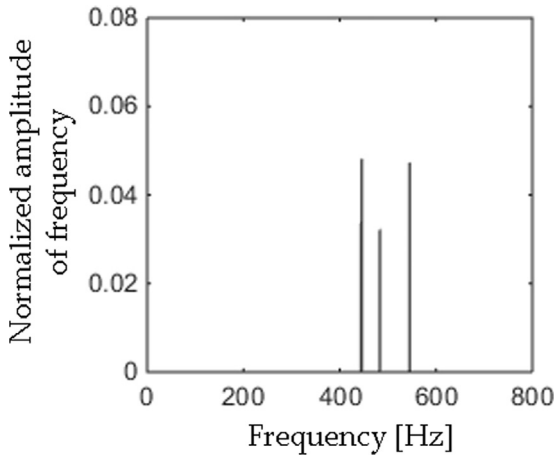


**Fig. 18.** Difference between frequency spectra of acoustic signals (|b-c|) using SMOFS-22-MULTIEXPANDED.

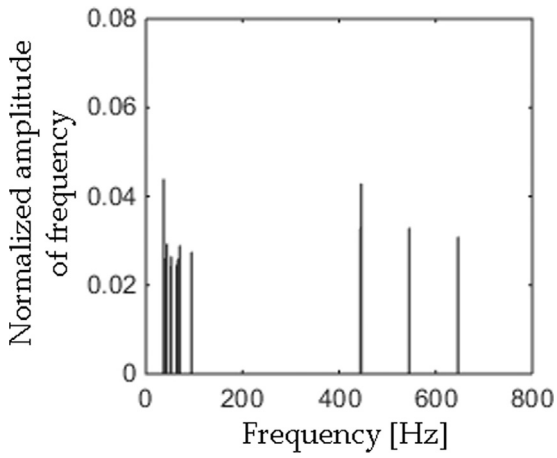


**Fig. 19.** Difference between frequency spectra of acoustic signals (|b-d|) using SMOFS-22-MULTIEXPANDED.

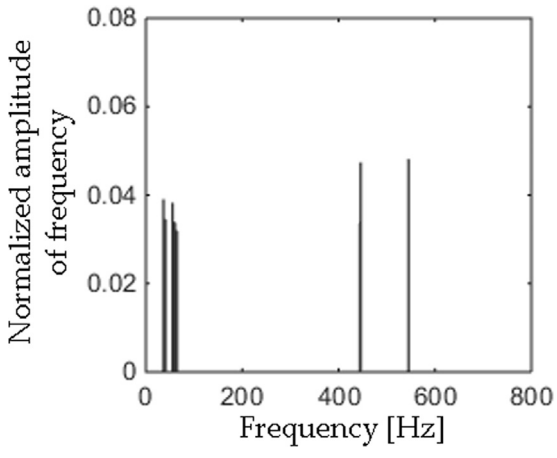


**Fig. 20.** Difference between frequency spectra of acoustic signals (|b-e|) using SMOFS-22-MULTIEXPANDED.

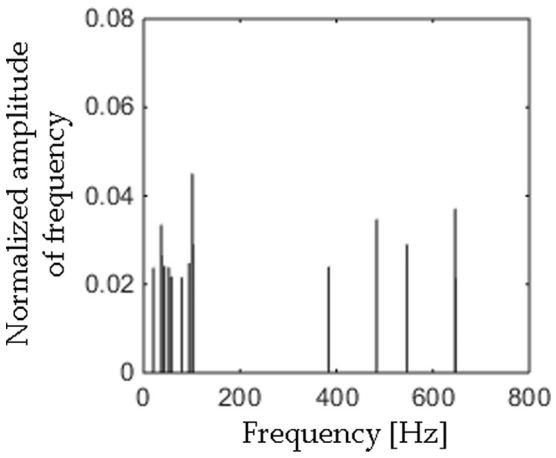


**Fig. 21.** Difference between frequency spectra of acoustic signals (|c-d|) using SMOFS-22-MULTIEXPANDED.

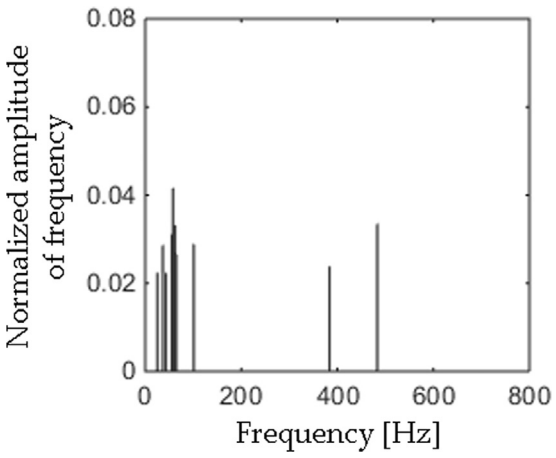


**Fig. 22.** Difference between frequency spectra of acoustic signals (|c-e|) using SMOFS-22-MULTIEXPANDED.

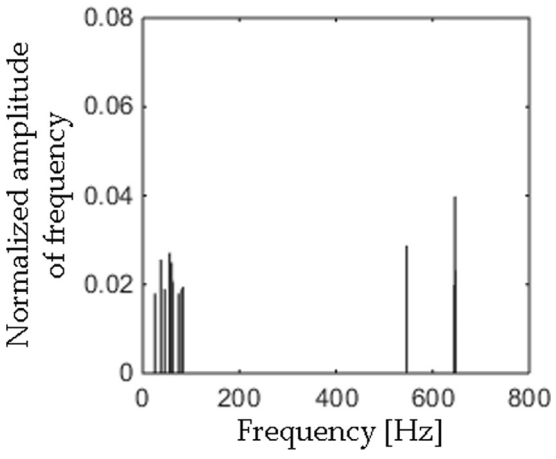


**Fig. 23.** Difference between frequency spectra of acoustic signals (|d-e|) using SMOFS-22-MULTIEXPANDED.

$$d(\mathbf{a},\mathbf{b}) = \sum_{i=1}^{1} |(a_i - b_i)|, \tag{4}$$

where test vector **a** and training vector **b** consisted of common frequency components. The similarity distances were computed for all analysed test and training vectors.

A more accurate description of the NN classifier is available in following articles [36–40].

## 3. Analysis of acoustic signals

Acoustic signals of motors were measured for 5 different states: healthy motor (Figs. 6, 10), motor with shorted coils of auxiliary winding and main winding (Fig. 7), motor with shorted coils of auxiliary winding (Fig. 8), motor with broken rotor bar and faulty ring of squirrel-cage (Fig. 9), motor with faulty bearing (Fig. 11). Motor parameters are defined as follows: $M_m$ = 3.3 kg, $V_{NM}$ = 230 V, $RS_M$ = 1390 rpm, $EC_N$ = 1.06 A, $EC_H$ = 0.5 A, $EC_{SA}$ = 1.8 A, $EC_{SM}$ = 4.5 A, $P_{NM}$ = 0.12 kW, $f_{NM}$ = 50 Hz, where $M_m$ – mass of the motor, $V_{NM}$ – nominal voltage of the motor, $RS_M$ – rotor speed of the motor, $EC_N$ – nominal electric current of the motor, $EC_H$ – electric current of the healthy motor, $EC_{SA}$ – electric current of the motor with shorted coils of auxiliary winding, $EC_{SM}$ – electric current of the motor with shorted coils of auxiliary winding and main winding, $P_{NM}$ – nominal power of the motor, $f_{NM}$ – nominal frequency of the motor.

The author used 20 one-second audio files for pattern creation and 200 one-second audio files for testing process (prediction phase). Training and test samples of acoustic signals of motors were analysed using proposed approach (Fig. 12a). Efficiency of recognition of acoustic signal was expressed as (5):

$$E_{RAS} = (N_{PTSAS})/(N_{ATSAS}) \cdot 100\% \tag{5}$$

where: $E_{RAS}$ – efficiency of recognition of acoustic signal of selected class, $N_{PTSAS}$ – number of test audio files of selected class tested properly, $N_{ATSAS}$ – number of all test audio files of selected class.

Total efficiency of recognition was defined as follows (6):

$$TE_{RAS} = (E_{RAS1} + E_{RAS2} + E_{RAS3} + E_{RAS4} + E_{RAS5})/5 \tag{6}$$

where $TE_{RAS}$ – total efficiency of recognition, $E_{RAS1}$ – efficiency of recognition of the healthy motor, $E_{RAS2}$ – efficiency of recognition of the motor with shorted coils of auxiliary winding and main winding, $E_{RAS3}$ – efficiency of recognition of the motor with shorted coils of auxiliary winding, $E_{RAS4}$ – efficiency of recognition of the motor with broken rotor bar and faulty ring of squirrel-cage, $E_{RAS5}$ – efficiency of recognition of the motor with faulty bearing.

The results of analysis of acoustic signals were shown in Tables 1–3. In the Table 1, the author presented the results of recognition of acoustic signals using the SMOFS-22-MULTIEXPANDED, *TCFC-MULTI* = 0.25 (found 14 common frequency components) and the NN classifier.

**Table 1**
Results of recognition of acoustic signals using the SMOFS-22-MULTIEXPANDED, *TCFC-MULTI* = 0.25, and the NN classifier.

| Type of acoustic signal | $E_{RAS}$ [%] |
|---|---|
| Healthy motor | 100 |
| Motor with shorted coils of auxiliary winding | 100 |
| Motor with shorted coils of auxiliary winding and main winding | 100 |
| Motor with broken rotor bar and faulty ring of squirrel-cage | 100 |
| Motor with faulty bearing | 85 |
| | $TE_{RAS}$ [%] |
| | 97 |

**Table 2**
Results of recognition of acoustic signals using the SMOFS-22-MULTIEXPANDED, *TCFC-MULTI* = 0.275, and the NN classifier.

| Type of acoustic signal | $E_{RAS}$ [%] |
|---|---|
| Healthy motor | 80 |
| Motor with shorted coils of auxiliary winding | 100 |
| Motor with shorted coils of auxiliary winding and main winding | 100 |
| Motor with broken rotor bar and faulty ring of squirrel-cage | 100 |
| Motor with faulty bearing | 90 |
| | $TE_{RAS}$ [%] |
| | 94 |

**Table 3**
The results of recognition of acoustic signals using the SMOFS-22-MULTIEXPANDED, *TCFC-MULTI* = 0.325, and the NN classifier.

| Type of acoustic signal | $E_{RAS}$ [%] |
|---|---|
| Healthy motor | 100 |
| Motor with shorted coils of auxiliary winding | 100 |
| Motor with shorted coils of auxiliary winding and main winding | 85 |
| Motor with broken rotor bar and faulty ring of squirrel-cage | 100 |
| Motor with faulty bearing | 92.5 |
| | $TE_{RAS}$ [%] |
| | 95.5 |

In the Table 2, the author presented the results of recognition of acoustic signals using the SMOFS-22-MULTIEXPANDED, *TCFC-MULTI* = 0.275 (found 8 common frequency components) and the NN classifier.

In the Table 3, the author presented the results of recognition of acoustic signals using the SMOFS-22-MULTIEXPANDED, *TCFC-MULTI* = 0.325 (found 4 common frequency components) and the NN classifier.

The conducted analysis provided very good results ($TE_{RAS}$ was in the range of 94%–97%). The SMOFS-22-MULTIEXPANDED computed 4–14 common frequency components. Computed vectors were used by the NN classifier. For industrial applications the results would be similar. The most important task is to create proper training and testing sets of acoustic signals of motors. Next the proposed method SMOFS-22-MULTIEXPANDED will find proper common frequency components for the analysis. It is very good method of feature extraction of acoustic signals of rotating electric motor. However more faults and motors should be analysed for maintenance purpose.

## 4. Conclusions

In this article the author described bearing, stator and rotor fault diagnostic methods of the single-phase induction motor. The proposed approach used acoustic signals. The author analysed acoustic signals of 5 states of the single-phase induction motor: healthy motor, motor with shorted coils of auxiliary winding and main winding, motor with shorted coils of auxiliary winding, motor with broken rotor bar and faulty ring of squirrel-cage, motor with faulty bearing. The SMOFS-22-MULTIEXPANDED was implemented as feature extraction method of acoustic signals. For the classification step the NN classifier was used. The obtained results of analysed approach were good ($TE_{RAS}$ was in the range of 94%–97%). The developed fault diagnostic approach was inexpensive. Low-cost capacity microphone and PC cost about 300$. Digital voice recorder also costs 100–300$. Measurement of acoustic signals is also immediate and non-invasive. Information provided from acoustic signals allow us to plan diagnostic review and repairs. The proposed signal processing methods can find application for early fault diagnosis of electrical and mechanical faults of rotating machines. The disadvantage of previously mentioned methods is that acoustic signals are mixed together (e.g. reflections, waves overlapping).

In the future, thermal, vibration and electrical signals of rotating machines will be analysed to improve proposed methods. Other faults and operating parameters of motors will be analysed. The more reliable fault diagnostic methods will be proposed, implemented and used for industry and electric vehicles.

## Acknowledgments

This work has been supported by AGH University of Science and Technology, grant no. 11.11.120.714.

## References

[1] P.L. Mendonca, E.L. Bonaldi, L.E.L. de Oliveira, G. Lambert-Torres, J.G.B. da Silva, L.E.B. da Silva, C.P. Salomon, W.C. Santana, A.H. Shinohara, Detection and modelling of incipient failures in internal combustion engine driven generators using electrical signature analysis, Electr. Power Syst. Res. 149 (2017) 30–45, https://doi.org/10.1016/j.epsr.2017.04.007.
[2] A.F. Aimer, A.H. Boudinar, N. Benouzza, A. Bendiabdellah, Use of the root-ar method in the diagnosis of induction motor's mechanical faults, Rev. Roum. Sci. Tech., Serie Electrotech. Energet. 62 (2) (2017) 134–141.
[3] S. Sakhara, S. Saad, L. Nacib, Diagnosis and detection of short circuit in asynchronous motor using three-phase model, Int. J. Syst. Assurance Eng. Manage. 8 (2) (2017) 308–317, https://doi.org/10.1007/s13198-016-0435-1.
[4] S. Choi, M.S. Haque, A.K.M. Arafat, H.A. Toliyat, Detection and estimation of extremely small fault signature by utilizing multiple current sensor signals in electric machines, IEEE Trans. Ind. Appl. 53 (3) (2017) 2805–2816, https://doi.org/10.1109/TIA.2017.2660463.
[5] L. Yu, Y.T. Zhang, W.Q. Huang, K. Teffah, A Fast-acting diagnostic algorithm of insulated gate bipolar transistor open circuit faults for power inverters in electric vehicles, Energies 10 (4) (2017), https://doi.org/10.3390/en10040552, Article Number: 552.
[6] A. Romanenko, A. Muetze, J. Ahola, Incipient bearing damage monitoring of 940-h variable speed drive system operation, IEEE Trans. Energy Convers. 32 (1) (2017) 99–110, https://doi.org/10.1109/TEC.2016.2618600.
[7] A. Glowacz, W. Glowacz, Z. Glowacz, Recognition of armature current of DC generator depending on rotor speed using FFT, MSAF-1 and LDA, Eksploatacja i Niezawodnosc-Maintenance Reliab. 17 (1) (2015) 64–69, https://doi.org/10.17531/ein.2015.1.9.
[8] J.A. Antonino-Daviu, K.N. Gyftakis, R. Garcia-Hernandez, H. Razik, A.J.M. Cardoso, Comparative influence of adjacent and non-adjacent broken rotor bars on the induction motor diagnosis through MCSA and ZSC methods, in: IECON 2015 – 41st Annual Conference of the IEEE Industrial Electronics Society, IEEE Industrial Electronics Society, Yokohama, Japan, 2015, pp. 1680–1685.

[9] T. Yang, H.B. Pen, Z.X. Wang, C.S. Chang, Feature knowledge based fault detection of induction motors through the analysis of stator current data, IEEE Trans. Instrum. Meas. 65 (2016) 549–558, https://doi.org/10.1109/TIM.2015.2498978.
[10] M. Gutten, D. Korenciak, M. Kucera, M. Sebok, M. Opielak, P. Zukowski, T.N. Koltunowicz, Maintenance diagnostics of transformers considering the influence of short-circuit currents during operation, Eksploatacja i Niezawodnosc-Maintenance Reliab. 19 (3) (2017) 459–466, https://doi.org/10.17531/ein.2017.3.17.
[11] M. Gutten, R. Janura, M. Sebok, D. Korenciak, M. Kucera, Measurement of short-circuit effects on transformer winding with SFRA method and impact test, Metrol. Measur. Syst. 23 (4) (2016) 521–529, https://doi.org/10.1515/mms-2016-0044.
[12] Z.X. Li, Y. Jiang, C. Hu, Z. Peng, Recent progress on decoupling diagnosis of hybrid failures in gear transmission systems using vibration sensor signal: a review, Measurement 90 (2016) 4–19, https://doi.org/10.1016/j.measurement.2016.04.036.
[13] A. Moosavian, G. Najafi, B. Ghobadian, M. Mirsalim, The effect of piston scratching fault on the vibration behavior of an IC engine, Appl. Acoust. 126 (2017) 91–100, https://doi.org/10.1016/j.apacoust.2017.05.017.
[14] E. Armentani, R. Sepe, A. Parente, M. Pirelli, Vibro-acoustic numerical analysis for the chain cover of a car engine, Appl. Sci.-Basel 7 (6) (2017), https://doi.org/10.3390/app7060610.
[15] M. Saimurugan, R. Ramprasad, A dual sensor signal fusion approach for detection of faults in rotating machines, J. Vib. Control 24 (12) (2018) 2621–2630, https://doi.org/10.1177/1077546316689644.
[16] S.L. Lu, P. Zhou, X.X. Wang, Y.B. Liu, F. Liu, J.W. Zhao, Condition monitoring and fault diagnosis of motor bearings using undersampled vibration signals from a wireless sensor network, J. Sound Vib. 414 (2018) 81–96, https://doi.org/10.1016/j.jsv.2017.11.007.
[17] D. Zurita-Millan, M. Delgado-Prieto, J.J. Saucedo-Dorantes, J.A. Carino-Corrales, R.A. Osornio-Rios, J.A. Ortega-Redondo, R.D. Romero-Troncoso, Vibration signal forecasting on rotating machinery by means of signal decomposition and neurofuzzy modeling, Shock Vib. (2016), https://doi.org/10.1155/2016/2683269, Article Number: 2683269.
[18] J.J. Saucedo-Dorantes, M. Delgado-Prieto, J.A. Ortega-Redondo, R.A. Osornio-Rios, R.D. Romero-Troncoso, Multiple-fault detection methodology based on vibration and current analysis applied to bearings in induction motors and gearboxes on the kinematic chain, Shock Vib. (2016), https://doi.org/10.1155/2016/5467643, Article Number: 5467643.
[19] J.A. Carino-Corrales, J.J. Saucedo-Dorantes, D. Zurita-Millan, M. Delgado-Prieto, J.A. Ortega-Redondo, R.A. Osornio-Rios, R.D. Romero-Troncoso, Vibration-based adaptive novelty detection method for monitoring faults in a kinematic chain, Shock Vib. (2016), https://doi.org/10.1155/2016/2417856.
[20] X. Yu, F. Dong, E.J. Ding, S.P. Wu, C.Y. Fan, Rolling bearing fault diagnosis using modified LFDA and EMD with sensitive feature selection, IEEE Access 6 (2018) 3715–3730, https://doi.org/10.1109/ACCESS.2017.2773460.
[21] G. Singh, T.C.A. Kumar, V.N.A. Naikan, Induction motor inter turn fault detection using infrared thermographic analysis, Infrared Phys. Technol. 77 (2016) 277–282, https://doi.org/10.1016/j.infrared.2016.06.010.
[22] D. Lopez-Perez, J. Antonino-Daviu, Application of infrared thermography to failure detection in industrial induction motors: case stories, IEEE Trans. Ind. Appl. 53 (3) (2017) 1901–1908, https://doi.org/10.1109/TIA.2017.2655008.
[23] O. Janssens, R. Schulz, V. Slavkovikj, K. Stockman, M. Loccufier, R. Van de Walle, S. Van Hoecke, Thermal image based fault diagnosis for rotating machinery, Infrared Phys. Technol. 73 (2015) 78–87, https://doi.org/10.1016/j.infrared.2015.09.004.
[24] G. Singh, V.N.A. Naikan, Infrared thermography based diagnosis of inter-turn fault and cooling system failure in three phase induction motor, Infrared Phys. Technol. 87 (2017) 134–138, https://doi.org/10.1016/j.infrared.2017.10.007.
[25] X.J. Chen, Y.M. Yang, Analysis of the partial discharge of ultrasonic signals in large motor based on Hilbert-Huang transform, Appl. Acoust. 131 (2018) 165–173, https://doi.org/10.1016/j.apacoust.2017.10.028.
[26] P. Sangeetha, S. Hemamalini, Dyadic wavelet transform-based acoustic signal analysis for torque prediction of a three-phase induction motor, IET Signal Proc. 11 (5) (2017) 604–612, https://doi.org/10.1049/iet-spr.2016.0165.
[27] M. Uekita, Y. Takaya, Tool condition monitoring for form milling of large parts by combining spindle motor current and acoustic emission signals, Int. J. Adv. Manuf. Technol. 89 (1–4) (2017) 65–75, https://doi.org/10.1007/s00170-016-9082-6.
[28] D.Y. Ning, J.Y. Hou, Y.J. Gong, Z.M. Zhang, C.L. Sun, Auto-identification of engine fault acoustic signal through inverse trigonometric instantaneous frequency analysis, Adv. Mech. Eng. 8 (3) (2016), https://doi.org/10.1177/1687814016641840, Article Number: 1687814016641840.
[29] R. Lara, R. Jimenez-Romero, F. Perez-Hidalgo, M.D. Redel-Macias, Influence of constructive parameters and power signals on sound quality and airborne noise radiated by inverter-fed induction motors, Measurement 73 (2015) 503–514, https://doi.org/10.1016/j.measurement.2015.05.049.
[30] E. Carletti, G. Miccoli, F. Pedrielli, G. Parise, Vibroacoustic measurements and simulations applied to external gear pumps. An integrated simplified approach, Arch. Acoustics 41 (2) (2016) 285–296, https://doi.org/10.1515/aoa-2016-0028.
[31] A. Stief, J.R. Ottewill, M. Orkisz, J. Baranowski, Two stage data fusion of acoustic, electric and vibration signals for diagnosing faults in induction motors, Elektron. Elektrotechn. 23 (6) (2017) 19–24, https://doi.org/10.5755/j01.eie.23.6.19690.
[32] M.R. Islam, J. Uddin, J.M. Kim, Acoustic emission sensor network based fault diagnosis of induction motors using a gabor filter and multiclass support vector machines, Ad Hoc Sens. Wirel. Networks 34 (1–4) (2016) 273–287.
[33] W.J. Wang, L.L. Cui, D.Y. Chen, Multi-scale morphology analysis of acoustic emission signal and quantitative diagnosis for bearing fault, Acta Mech. Sin. 32 (2) (2016) 265–272, https://doi.org/10.1007/s10409-015-0529-z.
[34] P.A. Delgado-Arredondo, D. Morinigo-Sotelo, R.A. Osornio-Rios, J.G. Avina-Cervantes, H. Rostro-Gonzalez, R.D. Romero-Troncoso, Methodology for fault detection in induction motors via sound and vibration signals, Mech. Syst. Sig. Process. 83 (2017) 568–589, https://doi.org/10.1016/j.ymssp.2016.06.032.
[35] A. Glowacz, Fault diagnostics of acoustic signals of loaded synchronous motor using SMOFS-25-EXPANDED and selected classifiers, Tehnicki Vjesnik-Technical Gazette 23 (5) (2016) 1365–1372, https://doi.org/10.17559/TV-20150328135652.
[36] I. Bandyopadhyay, P. Purkait, C. Koley, A combined image processing and nearest neighbor algorithm tool for classification of incipient faults in induction motor drives, Comput. Electr. Eng. 54 (2016) 296–312, https://doi.org/10.1016/j.compeleceng.2016.01.014.
[37] J. Tian, C. Morillo, M.H. Azarian, M. Pecht, Motor bearing fault detection using spectral kurtosis-based feature extraction coupled With K-nearest neighbor distance analysis, IEEE Trans. Ind. Electron. 63 (3) (2016) 1793–1803, https://doi.org/10.1109/TIE.2015.2509913.
[38] A. Glowacz, Acoustic based fault diagnosis of three-phase induction motor, Appl. Acoust. 137 (2018) 82–89, https://doi.org/10.1016/j.apacoust.2018.03.010.
[39] D.Y. Dou, S.S. Zhou, Comparison of four direct classification methods for intelligent fault diagnosis of rotating machinery, Appl. Soft Comput. 46 (2016) 459–468, https://doi.org/10.1016/j.asoc.2016.05.015.
[40] P. Baraldi, F. Cannarile, F. Di Maio, E. Zio, Hierarchical k-nearest neighbours classification and binary differential evolution for fault diagnostics of automotive bearings operating under variable conditions, Eng. Appl. Artif. Intell. 56 (2016) 1–13, https://doi.org/10.1016/j.engappai.2016.08.011.
[41] G.H. Bazan, P.R. Scalassara, W. Endo, A. Goedtel, W.F. Godoy, R.H.C. Palacios, Stator fault analysis of three-phase induction motors using information measures and artificial neural networks, Electr. Power Syst. Res. 143 (2017) 347–356, https://doi.org/10.1016/j.epsr.2016.09.031.
[42] Z.B. Hu, J. Su, V. Jotsov, O. Kochan, M. Mykyichuk, R. Kochan, T. Sasiuk, Data science applications to improve accuracy of thermocouples, in: 2016 IEEE 8th International Conference on Intelligent Systems (IS), 2016, pp. 180–188.
[43] O. Kochan, H. Sapojnyk, R. Kochan, Temperature field control method based on neural network, in: E.E. Daniel (Ed.), 2013 IEEE 7th International Conference on Intelligent Data Acquisition and Advanced Computing Systems (IDAACS 2013), 2013, https://doi.org/10.1109/IDAACS.2013.6662632.
[44] R.N. Liu, B.Y. Yang, E. Zio, X.F. Chen, Artificial intelligence for fault diagnosis of rotating machinery: a review, Mech. Syst. Sig. Process. 108 (2018) 33–47, https://doi.org/10.1016/j.ymssp.2018.02.016.
[45] F. Jia, Y.G. Lei, L. Guo, J. Lin, S.B. Xing, A neural network constructed by deep learning technique and its application to intelligent fault diagnosis of machines, Neurocomputing 272 (2018) 619–628, https://doi.org/10.1016/j.neucom.2017.07.032.

[46] Y. Lei, Intelligent Fault Diagnosis and Remaining Useful Life Prediction of Rotating Machinery, 2017, pp. 1–366. Document Type: Book.
[47] T. Waqar, M. Demetgul, Thermal analysis MLP neural network based fault diagnosis on worm gears, Measurement 86 (2016) 56–66, https://doi.org/10.1016/j.measurement.2016.02.024.
[48] D. Valis, L. Zak, Contribution to prediction of soft and hard failure occurrence in combustion engine using oil tribo data, Eng. Fail. Anal. 82 (2017) 583–598, https://doi.org/10.1016/j.engfailanal.2017.04.018.
[49] D. Valis, L. Zak, O. Pokora, P. Lansky, Perspective analysis outcomes of selected tribodiagnostic data used as input for condition based maintenance, Reliab. Eng. Syst. Saf. 145 (2016) 231–242, https://doi.org/10.1016/j.ress.2015.07.026.
[50] J.M. Johnson, A. Yadav, Complete protection scheme for fault detection, classification and location estimation in HVDC transmission lines using support vector machines, IET Sci. Meas. Technol. 11 (3) (2017) 279–287, https://doi.org/10.1049/iet-smt.2016.0244.
[51] C. Zhang, Z.X. Peng, S. Chen, Z.X. Li, J.G. Wang, A gearbox fault diagnosis method based on frequency-modulated empirical mode decomposition and support vector machine, Proc. Instit. Mech. Eng. Part C-J. Mech. Eng. Sci. 232 (2) (2018) 369–380, https://doi.org/10.1177/0954406216677102.
[52] X.P. Yan, X.J. Xu, C.X. Sheng, C.Q. Yuan, Z.X. Li, Intelligent wear mode identification system for marine diesel engines based on multi-level belief rule base methodology, Meas. Sci. Technol. 29 (1) (2018), https://doi.org/10.1088/1361-6501/aa966e.